Nano-scale distribution of ZnO free exciton luminescence in ZnO:Zn microcrystals and its modification under electron beam excitation

2006 J. Phys.: Condens. Matter 18 1967

(http://iopscience.iop.org/0953-8984/18/6/012)

INSTITUTE OF PHYSICS PUBLISHING JOURNAL OF PHYSICS: CONDENSED MATTER

J. Phys.: Condens. Matter **18** (2006) 1967–1975 doi:10.1088/0953-8984/18/6/012

Nano-scale distribution of ZnO free exciton luminescence in ZnO:Zn microcrystals and its modification under electron beam excitation

Masayoshi Ichimiya[1,2], Taku Horii[2], Takeshi Hirai[3], Yuji Sawada[2], Masaru Minamiguchi[1,2], Nobuhito Ohno[3], Masaaki Ashida[1,2] and Tadashi Itoh[1,2]

[1] CREST, Japan Science and Technology Agency, Japan
[2] Graduate School of Engineering Science, Osaka University, 1-3 Machikaneyama-cho, Toyonaka, Osaka 560-8531, Japan
[3] Academic Frontier Promotion Center, Osaka Electro-Communication University, 18-8 Hatsu-cho, Neyagawa, Osaka 572-8530, Japan

E-mail: ichimiya@laser.mp.es.osaka-u.ac.jp

Received 18 November 2005, in final form 8 January 2006
Published 25 January 2006
Online at stacks.iop.org/JPhysCM/18/1967

Abstract

The dependences of cathodoluminescence (CL) from ZnO:Zn phosphor powder upon local space, accelerating voltage and beam current have been investigated at room temperature. Ultraviolet (UV) luminescence, which is hard to be observed in photoluminescence (PL) at room temperature, has been clearly observed in CL as well as green luminescence. The intensity ratio of the UV luminescence to the green one varies from point to point. From the comparison with PL, the UV luminescence is attributed to the recombination of ZnO free excitons. The UV luminescence is little observed at low accelerating voltage where, similar to the excitation light for PL measurement, the electron beam penetrates into only the surface depletion layer where free excitons are unstable due to the surface electric field. However, the UV luminescence from the depletion layer becomes observable at large beam current because of the suppression of the electric field in the depletion layer caused by injected electrons.

1. Introduction

In recent years, wide band gap semiconductors have been studied with a great deal of attention for their potential applications in blue or ultraviolet (UV) light emitting devices. ZnO has a band gap of 3.37 eV and an exciton binding energy of 60 meV [1] which is larger than that in GaN (21–26 meV) and also larger than the thermal energy at room temperature.

Pure ZnO exhibits UV luminescence arising from the radiative recombination of excitons at room temperature [2]. Under high density excitation, there appear several nonlinear luminescence bands associated with exciton–exciton scattering and electron–hole plasma [3]. Since these luminescence bands have high optical gain, laser oscillation has been observed in epitaxially grown ZnO thin films [4].

On the other hand, ZnO powders tend to contain oxygen vacancies resulting in green luminescence [5]. ZnO particles in which many oxygen vacancies are intentionally introduced are called ZnO:Zn phosphor, a typical green phosphor for low-energy electron beam excitation [6]. In ZnO:Zn, the energy of excited electron–hole pairs is efficiently transferred to oxygen vacancies, which has been considered to quench the UV luminescence [7]. According to Vanheusden *et al* [5], the intensity of the green luminescence band strongly depended on the thickness of the depletion layer which arose from the transfer of electrons from the bulk or the oxygen vacancies to the surface states. As is the case with green luminescence, the UV luminescence might also be influenced by the existence of the depletion layer.

The cathodoluminescence (CL) imaging technique is extremely useful for assessing the spatial distribution of different radiative and nonradiative recombination sites in phosphor powders [8, 9]. By varying the accelerating voltage and current of the electron beam, one can control the penetration depth and the density of injected carriers [10]. Many researches on the CL of ZnO have been reported, while the UV luminescence efficiency is associated with only the crystalline quality in most cases [9, 11–25]. Therefore, only the green luminescence band has attracted interests for ZnO:Zn in CL as well as in photoluminescence (PL) where the UV luminescence is hard to be observed at room temperature [8, 26–28]. Little attention has been given to the UV luminescence of ZnO:Zn, although the improvement of the CL efficiency in the ZnO which contains many defects in the surface layer would be a great help in realizing linear or nonlinear optical devices which operate with high efficiency.

In the present study, we investigate the conditions needed for ZnO powder phosphor excitation to increase the UV luminescence efficiency in the case of lower material purity. For this purpose, we have measured spatially resolved CL spectra for the green and the UV luminescence bands in ZnO:Zn phosphor powders under different accelerating voltage and beam current at room temperature. For the comparison, we have also observed PL spectra in the UV region under different photoexcitation intensities.

2. Experimentals

Commercially sold ZnO:Zn phosphor powder was mixed with ethanol and dispersed on a brass sample holder. The sample was set in a field-emission-type scanning electron microscope (SEM) equipped with a CL measurement system. The accelerating voltage and the beam current of the SEM could be varied from 0.5 to 30 kV and from 7 pA to 10 nA, respectively. The CL from the sample was collected by an ellipsoidal mirror placed above the sample and sent through an optical fibre to a spectrometer equipped with a CCD. The CL intensity image consisted of 100×100 pixels and each pixel corresponded to an area of 63×63 nm^2. The intensity image for an arbitrary energy range could be obtained in addition to the spectrally integrated one. In the measurements of accelerating voltage and beam current dependences, the spatially averaged CL spectra were detected with an electron beam scanning the sample surface over an area of 300×300 nm^2 to reduce the CL quenching due to the damage to the sample by the electron beam irradiation. The spectral resolution was better than 10 meV.

The PL for low intensity excitation was measured with a He–Cd laser, and the PL for high intensity excitation was measured with the third harmonic light of a Nd^{3+}:YAG laser by varying the power between 1.7 and 680 kW cm^{-2}. These excitation lasers were incident on the sample

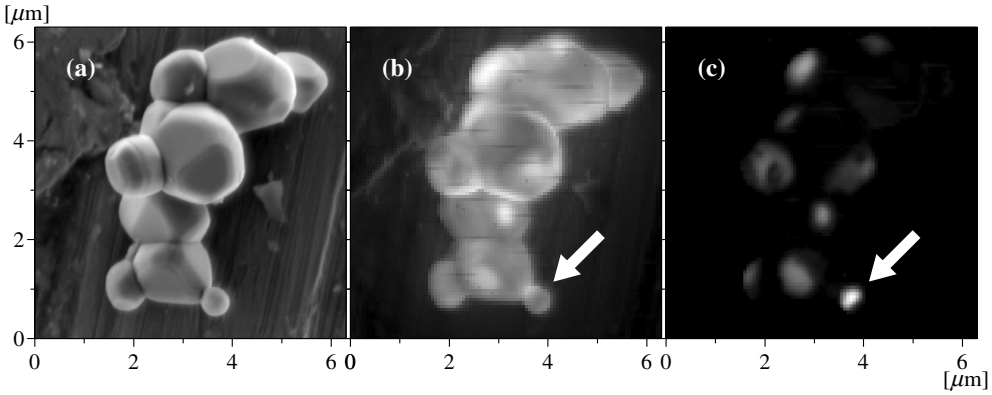

Figure 1. (a) SEM image of ZnO:Zn phosphor powders, (b) spectrally integrated CL intensity image of ZnO:Zn phosphor powders and (c) image of CL intensity of the UV band (3.0–3.5 eV) relative to that of the green band (1.8–2.8 eV). The accelerating voltage and beam current are 5.0 kV and 380 pA, respectively. White arrows indicate the smallest particle which shows UV luminescence with high efficiency.

with spot diameters of 2 mm (He–Cd laser) and 14 mm (Nd^{3+}:YAG laser); a large number of particles were excited simultaneously and spatially averaged spectra were obtained. The spectral resolutions were better than 7 meV. All of the CL and PL measurements were carried out at room temperature.

3. Results

Figure 1(a) shows the SEM image of somewhat aggregated ZnO:Zn microcrystals at an accelerating voltage of 5.0 kV and a beam current of 380 pA. The size of ZnO particles is distributed between 0.6 and 2 μm, and most particles show several crystal faces. The spectrally integrated CL intensity image of the same area as the SEM image is shown in figure 1(b). The CL intensity varies even within a particle as well as among particles, and tends to be large on planes oblique to the surface of the sample holder. The CL intensity image for a particular energy region is also derived from this measurement and that for the green luminescence band is almost the same as the spectrally integrated one, since the intensity of green luminescence is much larger than that of UV luminescence under these excitation conditions. Figure 1(c) shows an image of CL intensity for the UV luminescence band relative to that for the green one. The energy ranges are from 3.0 to 3.5 eV for UV luminescence and from 1.8 to 2.8 eV for green luminescence, respectively. The UV luminescence appears at the same spots as the bright ones in (b). This result suggests that multiple reflections inside the particle do not contribute to the enhancement of CL in (b) and (c), since the light is absorbed within 1 μm in the UV region [29] where the CL efficiency is more enhanced than that in the green region. The internal absorption might cause the suppression of CL efficiency under the condition that the electrons are injected into the particle plane parallel to the surface of the sample holder, i.e. perpendicular to the electron beam [10]. High efficiency UV luminescence is observed at the smallest particle indicated by white arrows in figures 1(b) and (c), where the intensity of green luminescence is small. According to these results and similar measurements for other particles, the efficiency of UV luminescence tends to be large on particles with submicrometre-scale diameter.

Figure 2 shows the dependence of CL spectra on the accelerating voltage for a ZnO:Zn particle with a diameter of 500 nm. The beam current is set to 50 pA but it depends slightly

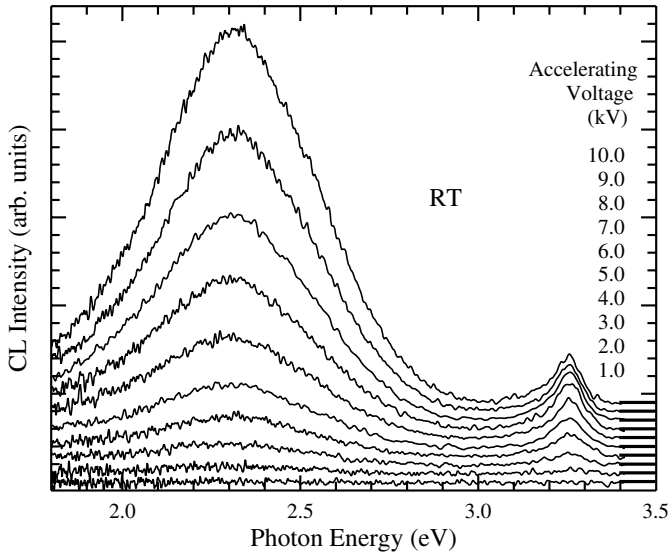

Figure 2. Accelerating voltage dependence of CL spectra of a ZnO:Zn particle. The spectral resolution is 9.3 meV at 3.3 eV.

on the voltage. Neither UV nor green luminescence is observed for an accelerating voltage of 1.0 kV. These luminescence bands appear above a voltage of 2.0 kV and increase with voltage, however the UV luminescence intensity seems to saturate above the voltage of 8.0 kV.

Figure 3(a) shows the dependence of the CL spectra on the beam current for the same particle. The accelerating voltage is fixed at 3.0 kV. No luminescence is observed at a beam current of 9.3 pA, while on increasing the current both UV and green luminescence bands appear and the CL intensity in the UV region relative to that in the green region increases in the large current region. Figure 3(b) shows the integrated CL intensities in the UV region (filled circles) and in the green region (open circles). In the small current region, the intensity of UV luminescence increases sublinearly, while above a current of 50 pA, it increases superlinearly and is proportional to the 1.4th power of the beam current. The intensity of the green luminescence increases linearly for almost all the range of the beam current.

For the PL spectra under He–Cd laser excitation, the UV luminescence is hardly observed, while it appears under intense excitation by the third harmonic light of a Nd^{3+}:YAG laser. Figure 4(a) shows the excitation power dependence of PL spectra in the UV region. The CL spectrum for a beam current of 330 pA shown in figure 3(a) is displayed again for comparison. The peak energies of the PL spectra are more than 80 meV lower than 3.291 eV for the CL peak and the energy slightly shifts to lower energy on increasing the excitation power. Figure 4(b) shows the excitation power dependence of the integrated intensity for the PL, where the intensity increases superlinearly and is proportional to the 1.6th power of the excitation intensity at the lower excitation level.

4. Discussion

In order to discuss the characteristic behaviour of the CL spectra in comparison with the PL spectra, the difference in luminescence properties between electron beam excitation and laser excitation should be considered. One important difference is the penetration depth of the injected electrons and of the incident photons. In photoexcitation, the penetration depth of

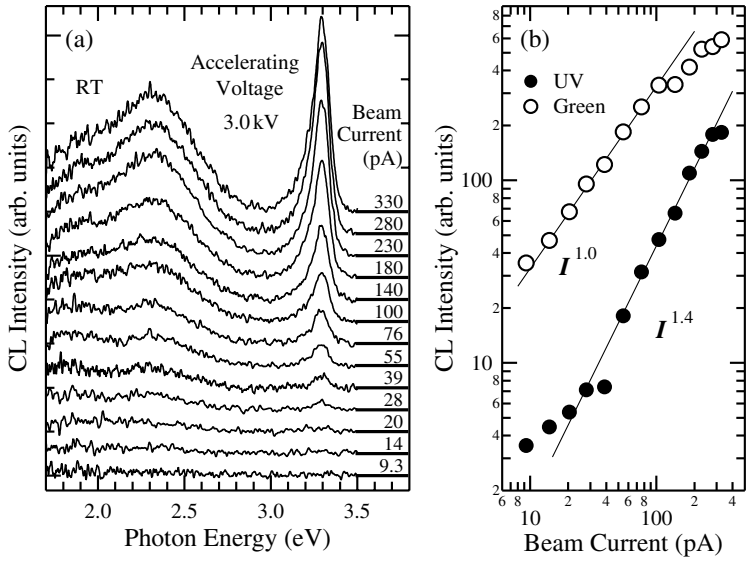

Figure 3. (a) Beam current dependence of CL spectra of a ZnO:Zn particle with an accelerating voltage of 3.0 kV. (b) The integrated intensities of the CL spectra versus the beam current. Filled and open circles indicate the intensities for UV and green bands, respectively.

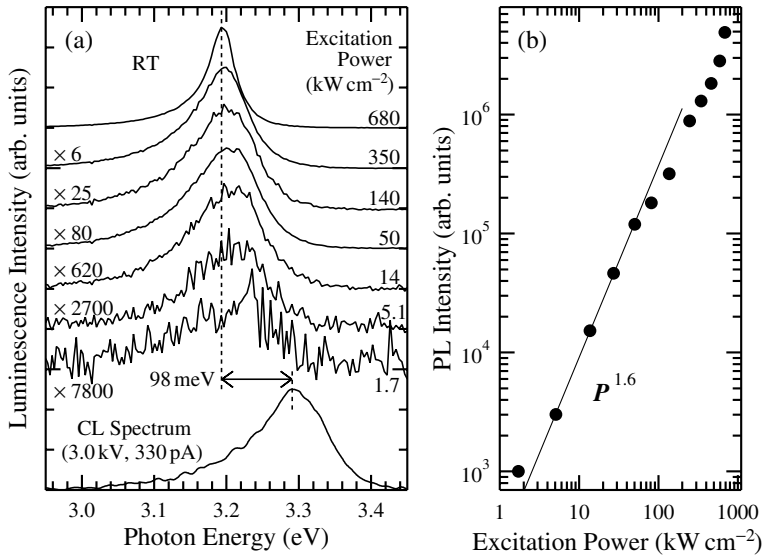

Figure 4. (a) Excitation power dependence of PL spectra. A typical CL spectrum is also shown for comparison. (b) The integrated intensity of the PL spectra versus the excitation power.

the photons with an energy of 3.49 eV is about 50 nm, which is determined from the absorption coefficient of 2×10^5 cm^{-1} [29]. In electron beam excitation, the penetration depth of electrons R_e (μm) is estimated from the relation [30]

$$R_e = \frac{2.76 \times 10^{-7} A E_b^{5/3}}{\rho Z^{8/9}} \frac{\left(1 + 0.978 \times 10^{-6} E_b\right)^{5/3}}{\left(1 + 1.957 \times 10^{-6} E_b\right)^{4/3}}, \tag{1}$$

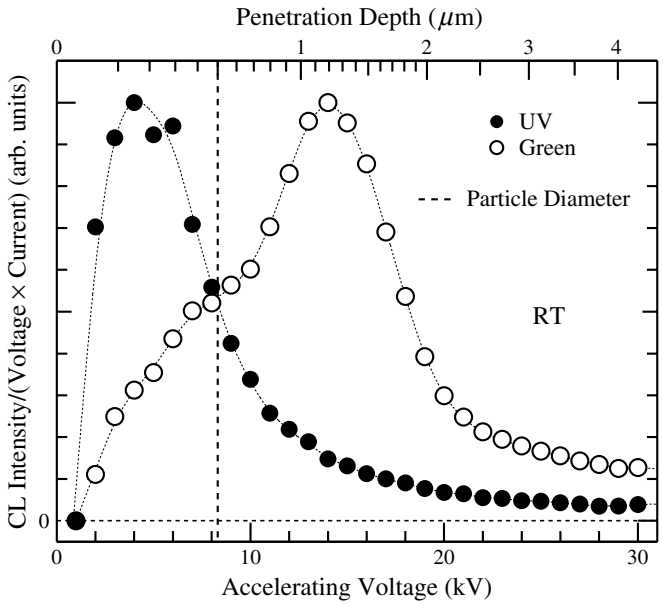

Figure 5. The integrated intensities of the UV and green luminescence bands in figure 2 versus the penetration depth calculated from the accelerating voltage. They are divided by the product of accelerating voltage and beam current and normalized at the peak. Filled and open circles indicate the intensities for UV and green bands, respectively. The vertical dashed line corresponds to the diameter of the ZnO:Zn particle.

where A, ρ, Z and E_b represent atomic weight (g mol^{-1}), density (g cm^{-3}), atomic number and kinetic energy of electrons (eV), respectively. In ZnO, ρ is 5.6 g cm^{-3}, and the average values of Zn and O are applied to A as 40.7 g mol^{-1} and Z as 19. The spatial spread of secondary electrons should be considered in addition to that of injected electrons for the estimation of excitation volume, while the penetration length for secondary electrons with the energy of a few eV is much less than that for injected electrons. Therefore, the excitation volume can be estimated from only the penetration depth of injected electrons, which is derived by substituting the values of accelerating voltage for E_b in equation (1) to be about 220 nm for an accelerating voltage of 5 kV and about 1.35 μm for 15 kV. Figure 5 shows the correlation between the penetration depth calculated from the accelerating voltage and the integrated CL intensity. Filled and open circles indicate the intensities for the UV and green bands, respectively. The dashed line at the penetration depth of 500 nm indicates the particle diameter derived from the SEM image. The number of excited carriers is considered to be in proportion to the accelerating voltage, since the CL intensity in the bulk crystal increases linearly with the accelerating voltage [31, 32]. Therefore, both intensities in figure 5 are divided by the product of accelerating voltage and beam current in order to emphasize the influence of changing the excitation volume on the CL efficiency. The UV luminescence efficiency increases with the penetration depth and becomes a maximum at a depth of between 91 nm (accelerating voltage of 3.0 kV) and 290 nm (6.0 kV). The luminescence efficiency decreases above 380 nm, where part of the injected electrons reaches near the reverse side of the particle. From this fact, the UV luminescence is considered to be generated in the core–particle region deeper than 50 nm corresponding to the penetration depth for photoexcitation. Here, the luminescence behaviour for a penetration depth more than 0.5 μm is explained as follows. The injected electrons with

a penetration depth more than the particle diameter reach the brass sample holder and the secondary electrons emitted from the holder excite the particle again. In the spatially resolved measurement shown in figure 1, the green luminescence band actually appears by injecting electrons into the position where ZnO:Zn particles are not observed in the SEM image. In the region of penetration depth beyond the particle diameter, the UV luminescence efficiency decreases monotonically. This result shows that the secondary electron does not contribute to the UV luminescence, since a secondary electron with lower kinetic energy hardly penetrates into the particle. On the other hand, the green luminescence still increases above the penetration depth corresponding to the particle diameter and is found to be generated by the secondary electron excitation. This fact suggests that most of the oxygen vacancies, which are the origin of green luminescence in ZnO:Zn, are distributed near the surface of the particle. The emission efficiency of the secondary electron is suppressed by too much penetration into the sample holder. The reduction of green luminescence efficiency above 14 kV in figure 5 reflects this feature. It should be noted that the penetration depth shown in figure 5 is calculated for ZnO and that for brass is somewhat smaller.

Next, another difference between photo- and electron-excitations is the order of excited electron–hole pair density. In the case of the PL measurement, the density is estimated to be 6×10^{17}–2×10^{20} cm^{-3} for an excitation power of 1.7–680 kW cm^{-2} from the absorption coefficient of 2×10^5 cm^{-1} [29] and the exciton lifetime of about 1 ns at room temperature [33]. As shown in figure 4, the PL intensity in this excitation power region increases superlinearly and the peak energy of the UV band is redshifted with increasing excitation power around 3.2 eV, which is about 0.1 eV lower than the peak position of the intrinsic exciton UV luminescence in pure ZnO [1]. In addition, the extreme enhancement and the reduction of the luminescence band width for 680 kW cm^{-2} in figure 4(a) indicate the onset of stimulated emission. From these features, the luminescence band observed in the PL measurement is attributed to the P band originating from inelastic exciton–exciton scattering in pure ZnO [4]. In the case of the CL measurement, the injected electron density is estimated to be 3.7×10^{13}–1.3×10^{15} cm^{-3} for a beam current of 9.3–330 pA and accelerating voltage of 3.0 kV, which corresponds to a penetration depth of 91 nm. The density of electron–hole pairs is larger than the injected electron density, since the mean energy of injected electrons is two orders of magnitude larger than that of the secondary electrons which contribute to the creation of electron–hole pairs. Nevertheless, the density for a beam current of 330 pA is estimated to be lower than 6×10^{17} cm^{-3} corresponding to that for the smallest power in the PL measurement.

The peak energy of the UV band in CL is almost the same as that of the free exciton luminescence of pure ZnO in the PL measurement [1, 3, 34, 35]. Moreover, the difference between the peak energies of the UV band in CL and the stimulated emission for photoexcitation at 680 kW cm^{-2} is 98 meV, as indicated in figure 4, which is equivalent to the difference between the P band with $n = \infty$ [4, 36]. In pure ZnO, longitudinal optical phonon (LO phonon) replicas of the free exciton appear below the energy of free exciton luminescence [12, 34, 35]. The low energy tail of the UV band in CL is associated with the LO phonon replicas which are thermally broadened.

Here, one has to consider the electronic states near the surface where no UV luminescence is observed. In recent years, Vanheusden *et al* [5] pointed out that the intensity of the green luminescence is influenced by the width of the depletion layer which depends on the number of surface states, the concentration of donor impurities and the size of the ZnO particle, because the transfer of electrons from the oxygen vacancies to the surface states directly affects the charge states of oxygen vacancies. Therefore, it is considered that the valence and conduction bands are bent within the depletion layer, resulting in the disappearance of excitons due to a strong electric field (Stark effect). The accelerating voltage dependence of CL spectra indicates

that the mean depletion depth of particles with diameters of 500 nm is larger than 50 nm, corresponding to the penetration depth for photoexcitation. In the PL measurement where only the depletion layer is excited, free exciton luminescence is not observed, while the internal field in the depletion layer is screened on increasing the density of photoexcited carriers, resulting in the appearance of the P band at the high density excitation [37]. Under electron beam excitation, however, it is possible to supply electrons to oxygen vacancies directly and suppress the internal field in the depletion layer differently from the case of photoexcitation. This effect may also cause the appearance of UV luminescence in the CL measurement for an accelerating voltage of 3.0 kV shown in figure 3 where most injected electrons only penetrate into the depletion layer.

5. Summary

Spatially resolved CL spectra of ZnO:Zn phosphor powders are investigated under different accelerating voltages and beam currents at room temperature. The UV luminescence intensity and its intensity ratio to the green luminescence vary among particles and even at different points inside each particle. From the comparison with the PL spectra under low and high intensity excitation conditions, it is strongly suggested that the UV luminescence is usually emitted from the internal region of the particles and only emitted from the surface region in the case that the electric field inside the depletion layer becomes weak enough and, therefore, the excitons become stable. In conclusion, the CL spectra of ZnO:Zn phosphors reflect clearly the spatial structure of phosphor, and the UV luminescence under electron beam excitation is attributed to the recombination of ZnO free excitons and is enhanced by injecting electrons into the core particle region or supplying electrons into the surface region with many oxygen vacancies.

Acknowledgment

This work was partially supported by the Grant-in-Aid for Scientific Research from the Ministry of Education, Culture, Sports, Science and Technology of Japan.

References

[1] Chen Y, Bagnall D M, Koh H, Park K, Hiraga K, Zhu Z and Yao T 1998 *J. Appl. Phys.* **84** 3912
[2] Zu P, Tang Z K, Wong G K L, Kawasaki M, Ohtomo A, Koinuma H and Segawa Y 1997 *Solid State Commun.* **103** 459
[3] Bagnall D M, Chen Y F, Zhu Z, Yao T, Shen M Y and Goto T 1998 *Appl. Phys. Lett.* **73** 1038
[4] Bagnall D M, Chen Y F, Zhu Z, Yao T, Koyama S, Shen M Y and Goto T 1997 *Appl. Phys. Lett.* **70** 2230
[5] Vanheusden K, Warren W L, Seager C H, Tallant D R, Voigt J A and Gnade B E 1996 *J. Appl. Phys.* **79** 7983
[6] Shionoya S 1999 *Phosphor Handbook* ed W M Yen (Boca Raton, FL: CRC Press)
[7] Ota T, Sasa S, Harada Y and Hashimoto S 2002 *Phys. Status Solidi* b **229** 815
[8] Tanaka S, Takahashi K, Sekiguchi T, Sumino K and Tanaka J 1995 *J. Appl. Phys.* **77** 4021
[9] Seager C H, Missert N A, Tallant D R and Warren W L 1998 *J. Appl. Phys.* **83** 1153
[10] Ong H C, Li A S K and Du G T 2001 *Appl. Phys. Lett.* **78** 2667
[11] Sekiguchi T, Ohashi N and Terada Y 1997 *Japan. J. Appl. Phys.* **36** L289
[12] Ohashi N, Sekiguchi T, Aoyama K, Ohgaki T, Terada Y, Sakaguchi I, Tsurumi T and Haneda H 2002 *J. Appl. Phys.* **91** 3658
[13] Jin Z W, Yoo Y Z, Sekiguchi T, Chikyow T, Ofuchi H, Fujioka H, Oshima M and Koinuma H 2003 *Appl. Phys. Lett.* **83** 39
[14] Alves H, Pfisterer D, Zeuner A, Riemann T, Christen J, Hofmann D M and Meyer B K 2003 *Opt. Mater.* **23** 33

[15] Hichou A E, Addou M, Bougrine A, Dounia R, Ebothe J, Troyon M and Amrani M 2004 *Mater. Chem. Phys.* **83** 43
[16] Yoo Y Z, Sekiguchi T, Chikyow T, Kawasaki M, Onuma T, Chichibu S F, Song J H and Koinuma H 2004 *Appl. Phys. Lett.* **84** 502
[17] Chen Z Q, Maekawa M, Yamamoto S, Kawasuso A, Yuan X L, Sekiguchi T, Suzuki R and Ohdaira T 2004 *Phys. Rev.* B **69** 035210
[18] Wang G, Zhang G, Ketterson J B and Gatt R 2004 *Thin Solid Films* **460** 232
[19] Chatterjee A, Shen C H, Ganguly A, Chen L C, Hsu C W, Hwang J Y and Chen K H 2004 *Chem. Phys. Lett.* **391** 278
[20] Saito N, Haneda H, Sekiguchi T, Ishigaki T and Koumoto K 2004 *J. Electrochem. Soc.* **151** H169
[21] Bertram F, Forster D, Christen J, Oleynik N, Dadgar A and Krost A 2004 *J. Cryst. Growth* **272** 785
[22] Lorenz M, Hochmuth H, Lenzner J, Nobis T, Zimmermann G, Diaconu M, Schmidt H, Wenckstern H V and Grundmann M 2005 *Thin Solid Films* **486** 205
[23] Panin G N, Baranov A N, Oh Y-J, Kang T W and Kim T W 2005 *J. Cryst. Growth* **279** 494
[24] Mei Y F, Siu G G, Fu R K Y, Wong K W, Chu P K, Lai C W and Ong H C 2005 *Nucl. Instrum. Methods* B **237** 307
[25] Takkouk Z, Brihi N, Guergouri K and Marfaing Y 2005 *Physica* B **366** 185
[26] Nakanishi Y, Miyake A, Kominami H, Aoki T, Hatanaka Y and Shimaoka G 1999 *Appl. Surf. Sci.* **142** 233
[27] Bondar V 2000 *Mater. Sci. Eng.* B **69/70** 505
[28] Lin C H, Chiou B S, Chang C H and Lin J D 2002 *Mater. Chem. Phys.* **77** 647
[29] Yoshikawa H and Adachi S 1997 *Japan. J. Appl. Phys.* **36** 6237
[30] Kanaya K and Okayama S 1972 *J. Phys. D: Appl. Phys.* **5** 43
[31] Kingsley J D and Prener J S 1972 *J. Appl. Phys.* **43** 3073
[32] Ozawa L 1983 *Appl. Phys. Lett.* **43** 1073
[33] Koida T, Chichibu S F, Uedono A, Tsukazaki A, Kawasaki M, Sota T, Sagawa Y and Koinuma H 2003 *Appl. Phys. Lett.* **82** 532
[34] Teke A, Özgür Ü, Doğan S, Gu X, Morkoç H, Nemeth B, Nause J and Everitt H O 2004 *Phys. Rev.* B **70** 195207
[35] Shan W, Walukiewicz W, Ager J W III, Yu K M, Yuan H B, Xin H P, Cantwell G and Song J J 2005 *Appl. Phys. Lett.* **86** 191911
[36] Kligshirn C 1975 *Phys. Status Solidi* b **71** 547
[37] Kuokstis E, Yang J W, Simin G, Khan M A, Gaska R and Shur M S 2002 *Appl. Phys. Lett.* **80** 977